High-thorium monazite-(Ce) formed during disequilibrium melting of metapelites under granulite-facies conditions

GORDON R. WATT

Geology & Cartography Division, School of Construction & Earth Sciences, Oxford Brookes University, Headington, Oxford, OX3 0BP, UK

Abstract

Monazite is a light rare-earth element (*LREE*)-bearing accessory phase common in felsic granitic rocks, and strongly influences *LREE* concentrations in granites and the chemistry of melts and residues formed during partial melting. Cheralite-rich (high-Th) monazite-(Ce) has been recorded as rims on partially dissolved cores in a suite of granulite-facies migmatites generated by disequilibrium melting. High-Th monazite has previously been recorded only in granitic-pegmatite occurrences. Subidiomorphic monazite-(Ce) from leucosome, melanosome and mesosome consists of complexly zoned cores (up to 300 μm in diameter) containing 5.17–9.87 wt.% ThO_2, overgrown by essentially unzoned rims (containing up to 21.4 wt.% ThO_2). Uranium contents are average for Th-rich monazite-(Ce) (0.22–3.17 wt.% UO_2). Th enrichment (relative to *LREE*) in monazite-(Ce) rims is ascribed to the presence of fluorine-bearing melts (formed during the incongruent breakdown of biotite to produce a water-undersaturated melt), allowing the formation of *REE*-fluoride complexes in the melt, coupled with the increased charge balanced substitutions $Th^{4+} + Si^{4+} \rightleftharpoons REE^{3+} + P^{5+}$ and $Th^{4+} + Ca^{2+} \rightleftharpoons 2REE^{3+}$ into monazite-(Ce). Fractionation of Th and U (reflected by an increased in Th/U in rims relative to cores) may have occurred due to the removal by a CO_2-rich fluid phase in the melt. These interpretations are consistent with elevated CO_2 and F contents of granitic liquids produced during the water-undersaturated breakdown of biotite under granulite-facies conditions. Evidence for restricted monazite-(Ce)–melt equilibration and rapid melt removal is provided by the ubiquitous presence of partially embayed cores and unzoned rims.

KEYWORDS: thorium, monazite, granulite facies, *REE*.

Introduction

MONAZITE-(Ce) $(Ce,La,Th)PO_4$ is the most common rare-earth element-bearing phosphate in S-Type granites, leucogranites and leucosomes in metapelitic migmatites (Miller, 1985; White, 1990). The concentrations of light rare-earth elements (*LREE*) in these felsic plutonic rocks are almost completely dominated by accessory phases such as monazite (Sawka *et al.*, 1984), making it a useful petrogenetic indicator in the study of *REE* chemistry in granitic lithologies. A SIMS mass-balance study of the Strontian Granodiorite (Hinton and Paterson, 1994) showed that up to 90% of the *LREE* were hosted in monazite. These high concentrations of *LREE* in monazite have led several authors to propose models for *LREE* depletion/enrichment of granitic magmas involving monazite-(Ce) fractionation and/or entrainment (Miller and Mittlefehldt, 1983; Wall and Harley, 1993; Zhao and Cooper, 1993). Furthermore, monazite is an important mineral in several isotopic systems (Sm/Nd; U/Pb; Th/Pb; Montel, 1993). Growth and fractionation of monazite may produce variations in garnet Sm/Nd, generating anomalously old Nd model ages (Sevigny, 1993) while Hensen and Zhou (1994) demonstrated that small amounts of microscopic to submicroscopic monazitc inclusions in garnet (0.01–0.001 wt.%) may be sufficient to cause anomalous Sm-Nd ages.

Monazite has the basic formula $(Ce,La,Th)PO_4$. Although typical Th contents are in the range 4–12% ThO_2 Th-rich monazite-(Ce) (cheralite) has been

Mineralogical Magazine, December 1995, Vol. 59, pp. 735–743

recorded from pegmatitic rocks (Grammacioli and Segalstad, 1978; Bowles *et al.*, 1980), and may contain up to 30% ThO_2. Charge-balanced Th substitution occurs through the following reactions:

$$Th^{4+} + Si^{4+} \rightleftharpoons REE^{3+} + P^{5+}, \text{ and} \quad (1)$$

$$Th^{4+} + Ca^{2+} \rightleftharpoons 2REE^{3+}. \quad (2)$$

The displacement of *REE* from monazite by substitution of Th may enhance melt *LREE* contents, especially in siliceous granitic melts (e.g. leucogranites). Uranium also substitutes into monazite — the most U-rich monazite recorded contains 15.64 wt.% UO_2 (Mannucci *et al.*, 1986) — and generally shows a positive correlation with Th. In addition to Th and U, further substitution of *LREE* and *MREE* elements (up to Gd or Tb) into the (La,Ce) position means a wide range of compositions can occur, depending on the activities of individual elements in the melt at the time of crystallization.

Th and U enrichment has generally been considered a feature of pegmatite-precipitated monazite, with the implication that enrichment in these elements is controlled, at least in part, by processes involving magmatic fluids. This paper provides the first example of high-Th monazite-(Ce) from migmatitic granitic rocks. This paper presents electron-microprobe analyses and X-ray elemental maps of Th-rich monazite-(Ce) in a suite of migmatites from eastern Antarctica (containing up to 23 wt.% ThO_2) from granitic leucosomes (and their host metapelitic gneisses and melanosomes) in granulite-facies migmatites and determines whether the high-Th contents represent a fluid-related feature or are a product of a melt-related process. The implications of these findings for models of melt–fluid evolution during partial melting under granulite-facies disequilibrium conditions are discussed.

Geological background

The Brattstrand Bluffs Coastline lies on the southern coast of Prydz Bay, eastern Antarctica (Harley and Hensen, 1990). Peak granulite metamorphism at approximately 6 kbar and 860°C was accompanied by the development of pervasive flat-lying foliations, followed by near isothermal decompression to 3–4 kbar, 700°C (Fitzsimons and Harley, 1991). The high-*T* clockwise *P–T* evolution of the Brattstrand Bluffs coastline has been interpreted in terms of an extensional collapse of thickened crust with increased heat-flow due to convective thinning of the underlying mantle lithosphere (Fitzsimons, 1991; Harley and Fitzsimons, 1991). Water-undersaturated partial melting involving the incongruent breakdown of biotite in reactions occurred at or near the metamorphic peak.

The retention of accessory phases (monazite and zircon) in melanosomes during partial melting led to the generation of low *LREE*, low-Th melts with disequilibrium chemistry (summarized in Watt and Harley, 1993). Mass-balance calculations show that melts were extracted before equilibration with their host melanosomes due to the restricted solubility of monazite-(Ce) in dry (water-undersaturated) peraluminous granitic melt. A combination of melt extraction before equilibration, concentration of partially dissolved monazite-(Ce) in the residue, and entrainment of melanosome material in (high melt fraction) leucosomes has led to the formation of a migmatite suite containing individual components (leucosome, mesosome (metapelitic gneiss) and melanosome) whose *LREE* chemistry is constrained almost solely by monazite-(Ce).

Analytical methods

Major element concentrations of monazite-(Ce) were obtained by wavelength dispersive electron probe microanalysis using a Cameca Camebax Microbeam microprobe at the Department of Geology and Geophysics, University of Edinburgh. Analyses were performed at an accelerating voltage of 20 kV and a beam current of approximately 20 nA. Absolute abundances for each element were determined by comparison of X-ray count data with synthetic glasses standards doped with *REE*. Correction for matrix effects was by an on-line PAP correction program. Counting times at peak and background spectrometer positions were 30 and 15 s respectively. X-ray maps were produced on a JEOL JSM-840 Scanning Electron Microscope at the Department of Geology, Oxford Brookes University. The maps were generated using LINK X-Ray Mapping Software, operating at a beam current of 2 nA and an accelerating voltage of 20 kV. The 14 frame 256 × 256 pixel images were collected using a dwell time of 40 ms (corrected for dead-time) and a spectrometer process time of 4 (for 1500–5000 X-ray counts per second).

Mineral chemistry

Backscattered electron imaging and X-ray mapping has identified strongly zoned and corroded monazite-(Ce) cores rimmed by unzoned overgrowths (Fig. 1), or, more rarely, by rims with only a slight amount of zoning and secondary embayment. Cores of monazite-(Ce) may reach 300 μm in diameter with subidiomorphic unzoned rims of varying width (typically <50 μm). Core zoning varies from complex to almost euhedral, but is often truncated by overgrowths. Rounded embayments and truncation of core zones show that partial dissolution of the

monazite-(Ce) occurred before reprecipitation of the overgrowths. Rims may be as narrow as 10 μm, but are always present.

Representative analyses of monazite-(Ce) compositions from the Brattstrand Bluffs Migmatites are given in Table 1, and selected literature values from granitic and pegmatitic occurrences in Table 2.

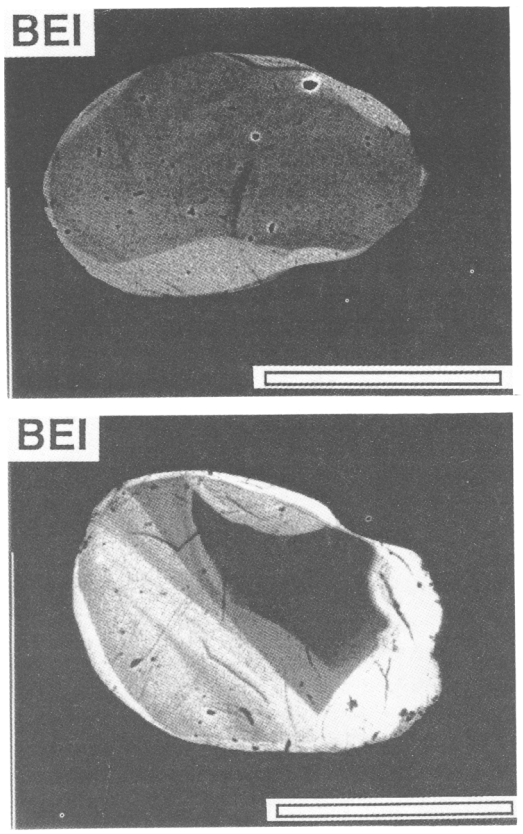

FIG. 1. (*a*) Back-scattered electron image of a large monazite-(Ce) grain in melanosome sample 58. The core shows well developed zoning caused by variations of 1–2 wt.% ThO_2 (and associated substitutions). Lobate embayments on the margin of the rim and sharp truncations of core zoning are evidencc for magmatic dissolution before reprecipitation of the unzoned, light coloured Th-rich rim. The rim contains up to 16 wt.% ThO_2, compared with a maximum core composition of 6.13 wt.% ThO_2. Scale bar 150 μm. (*b*) BEI and (*c*) X-ray maps of Th distribution in monazite-(Ce) grains from leucogneiss sample 122. Bright rims reflect high Th count rates, reflecting high rim ThO_2 contents. Marked Th zoning in the core is evident. Scale bar 100 μm.

Monazite-(Ce) cores in all three lithologies from the Brattstrand Bluffs migmatites (melanosome, metapelitic gneiss and leucogneiss) are relatively similar in composition to typical granitic monazite-(Ce) (Fig. 2). In these cores Ce_2O_3 contents range from 28.09 wt.% to 31.64 wt.%, and Th concentrations are relatively low (minimum ThO_2 = 5.17 wt.%, maximum = 9.87 wt.%). A strong negative correlation between Ca + Th cations (normalized to 16 oxygens) and La + Ce + Nd cations (normalized to 16 oxygens) suggests that coupled Ca + Th substitution for *LREE* occurred (e.g. reaction 2) (Fig. 3). Si contents are variable, although relatively high compared to literature values for pegmatitic monazite-(Ce) (e.g. analyses 6 and 7, Table 2) and are typically higher in overgrowths. Core P_2O_5 contents are higher, consistent with $Th^{4+} + Si^{4+} \rightleftharpoons REE^{3+} + P^{5+}$. Uranium contents are average for Th-rich monazite-(Ce), ranging from 0.22 to 3.17 wt.% UO_2, and are highest in Th-rich rims. The similarity between monazite-(Ce) core compositions (Table 1) in the melanosomes, leucogneisses and metapelitic gneisses and granitic monazites (Table 2) suggests that the embayed and rounded monazite-(Ce) cores may have come from a granitic precursor and have experienced at least one erosionary cycle.

Monazite-(Ce) overgrowths show a greater range of compositions than monazite-(Ce) cores. They are unusually thorogenic; the most Th-rich monazite-(Ce) overgrowths are found in metapelitic gneisses and contain up to 21.41 wt.% ThO_2. Monazite-(Ce) cores in the same grain contain only 9.87 wt.% ThO_2. This strong enrichment of Th in overgrowths is seen in all monazite-(Ce)-bearing lithologies, although the degree of enrichment is variable. Th contents are typically lower in overgrowths on monazite-(Ce) in leucogneisses than in metapelitic gneiss monazite-(Ce) rims. The increase in Th is accompanied by higher Ca and Si contents in the overgrowths, by

TABLE 1. Monazite compositions from the Brattstrand Bluffs migmatites

Sample	58	60	46A	122	112	147	60	46A	112	122	147	147
Lithology	*MEL core	MEL core	MEL core	LG core	LG core	MPG core	MEL rim	MEL rim	LG rim	LG rim	MPG rim	MPG rim
SiO_2	1.20	0.60	1.39	1.25	1.42	0.56	2.49	3.30	2.83	3.49	1.72	1.90
CaO	0.38	0.95	0.38	0.26	0.49	0.83	1.32	0.29	0.50	0.44	0.73	0.70
P_2O_5	27.38	28.57	26.92	27.62	26.81	27.85	25.27	24.06	23.90	24.60	26.17	25.49
UO_2	0.37	1.77	0.42	0.74	0.88	1.86	0.38	0.22	0.64	0.83	3.04	3.17
ThO_2	6.13	5.17	7.55	8.33	9.87	9.61	16.78	15.56	15.31	14.70	20.13	21.41
La_2O_3	13.23	13.52	15.24	16.47	15.32	13.35	10.95	13.62	12.40	11.91	10.90	10.28
Ce_2O_3	31.64	28.09	29.52	30.54	29.98	28.20	25.66	27.68	27.58	27.27	23.23	23.12
Pr_2O_3	3.27	2.53	2.82	2.59	2.59	2.50	2.28	2.42	2.45	2.57	1.99	1.74
Nd_2O_3	13.62	11.43	11.88	10.31	10.10	10.39	11.66	10.57	11.23	11.11	8.64	8.58
Sm_2O_3	1.40	1.52	0.94	0.73	0.78	1.47	1.08	0.60	0.85	0.93	0.95	0.80
Gd_2O_3	0.49	0.99	0.34	0.19	0.27	0.73	0.09	n.d.	0.02	0.22	0.31	0.37
Dy_2O_3	0.05	0.51	0.25	0.16	0.09	0.20	0.14	0.08	0.08	0.10	0.22	0.25
Total	99.15	95.64	97.63	99.20	98.59	97.54	98.11	98.39	97.78	98.19	98.02	97.79
Cations normalized for 16 oxygens												
Si	0.20	0.10	0.23	0.20	0.23	0.09	0.42	0.56	0.48	0.58	0.29	0.32
Ca	0.07	0.16	0.07	0.13	0.15	0.33	0.24	0.05	0.12	0.15	0.54	0.57
P	3.76	3.91	3.74	3.78	3.72	3.85	3.57	3.43	3.44	3.46	3.66	3.60
U	0.01	0.06	0.02	0.01	0.02	0.03	0.01	0.01	0.02	0.02	0.03	0.03
Th	0.23	0.19	0.28	0.31	0.37	0.36	0.64	0.60	0.59	0.56	0.76	0.81
La	0.79	0.81	0.92	0.98	0.93	0.80	0.67	0.85	0.78	0.73	0.66	0.63
Ce	1.88	1.66	1.77	1.81	1.80	1.69	1.57	1.71	1.72	1.66	1.41	1.41
Pr	0.19	0.15	0.17	0.15	0.16	0.15	0.14	0.15	0.15	0.16	0.12	0.11
Dy	0.00	0.03	0.01	0.01	0.01	0.01	0.01	0.00	0.00	0.01	0.01	0.01
Nd	0.79	0.66	0.70	0.60	0.59	0.61	0.69	0.64	0.68	0.66	0.51	0.51
Sm	0.08	0.09	0.05	0.04	0.04	0.08	0.06	0.04	0.05	0.05	0.05	0.05
Gd	0.03	0.05	0.02	0.01	0.02	0.04	0.01	–	0.02	0.01	0.02	0.02
Total	8.03	8.00	8.02	8.02	8.03	8.05	8.01	8.01	8.05	8.03	8.05	8.07
Th/U	17.38	2.97	18.80	34.00	20.44	11.90	45.43	74.50	31.16	34.69	28.04	31.27

n.d. — Not detected

* MEL — Melanosome
MPG — Metapelitic Gneiss

LG — Leucogneiss

TABLE 2. Typical granitic and pegmatitic monazite compositions

	1	2	3	4	5	6	7	8
SiO_2	2.29	1.82	0.86	0.03	2.08	0.6	0.8	0.16
CaO	2.79	<0.05	1.31	0.68	5.99	3.9	3.3	4.45
P_2O_5	29.73	24.9	28.10	29.28	27.10	28.4	30.0	31.02
Y_2O_3	2.33	0.15	1.05	1.08	0.08	0.6	2.7	1.01
UO_2	2.81	0.18	0.46*	0.16*	4.33	1.2	1.6	15.64
ThO_2	7.54	2.1	7.20	3.95	31.64	22.50	19.5	11.34
La_2O_3	9.79	14.2	14.10	15.38	12.12	13.7	9.6	13.89
Ce_2O_3	23.05	28.1	27.90	29.46	5.19	21.7	19.6	16.31
Pr_2O_3	2.90	4.08	2.80	–	1.20	1.4	2.5	1.64
Nd_2O_3	11.18	15	10.10	10.91	5.91	3.6	4.5	2.34
Sm_2O_3	3.01	1.34	1.75	1.59	1.81	1.1	5.4	–
Gd_2O_3	2.13	<0.2	1.73	0.88	0.45	1.1	2.0	–
Dy_2O_3	–	–	0.70	–	0.06	–	–	0.05
Total	99.55	91.87	97.60	93.24	97.96	99.80	101.50	97.85

* U_3O_8

1 Macusani monazite (Montel, 1993)
2 Monazite, Murvey Granite, Connemara (Feeley *et al.*, 1989)
3 Monazite, Dartmoor Granite, Cornwall (Ward *et al.*, 1992)
4 Monazite, Sweetwater Wash Pluton, California (Wark and Miller, 1993)
5 Cheralite, Kerala, India (Bowles *et al.*, 1980)
6 Average of 8 pegmatite monazites, Val Vigezzo, Italy (Demartin *et al.*, 1991)
7 Average of 8 pegmatite monazites, Arvogno, Val Vigezzo, Italy (Mannuci *et al.*, 1986)
8 U-rich monazite, Piona, Italy (Gramaccioli and Segalstad, 1978)

slightly higher UO_2 concentrations (notably in the metapelitic gneisses) and by lower P and *LREE* concentrations as predicted by the charge-balanced substitution reactions 1 and 2 shown above. Ce_2O_3 contents in overgrowths vary from 23.12 wt.% to 27.68 wt.% and show a strong negative correlation with ThO_2.

Fluid composition and Th–*REE* fractionation

Experimental work Keppler and Wyllie, 1990, 1991; Mysen and Virgo, 1985) has shown that chemical fractionation of certain elements can occur in fluids containing C-O-H-F and Cl. Partition coefficients for Th and U are very low when H_2O is the only volatile species present, so fluid-related processes will not fractionate Th and U during partial melting under amphibolite-facies conditions (where melts are water-saturated). Under granulite-facies conditions however, melts are undersaturated with respect to H_2O, and are relatively CO_2-rich. Th is not affected by CO_2-rich fluids, but U can be (Keppler and Wyllie, 1990) so a possible mechanism for fractionation of Th and U during granulite-facies melting exists.

The volatile species involved in the water-undersaturated melting of the Brattstrand Bluffs migmatites were dominated by C, O and H. The breakdown of biotite during incongruent melting produces an aqueous component, while organic matter in the metapelitic protoliths provides a source for carbon. The water-undersaturated melts of the Brattstrand Bluffs coastline contained carbon, evidenced by the presence of graphite as an accessory phase in both metapelitic gneisses and leucogneisses (Harley *et al.*, 1992; Fitzsimons, 1991). This carbon has a dominantly biogenic source ($\delta^{13}C = -15$ to -25 ‰, rather than a mantle origin. The addition of CO_2 before peak metamorphic conditions were attained would lower the a_{H_2O} of the system (effectively increasing the temperature of the liquidus at any given P and T), inhibiting melting. By increasing a_{CO_2} by progressive dissolution and extraction of H_2O in a water-undersaturated melt small amounts of graphite could easily be precipitated during melting, leading to a preferential enrichment of Th relative to U in remaining melts. Rim Th/U ratios are 3–4 times greater than core values in some samples (Table 1) indicating that Th enrichment due to U removal by a CO_2-rich fluid phase in the melt may be a plausible

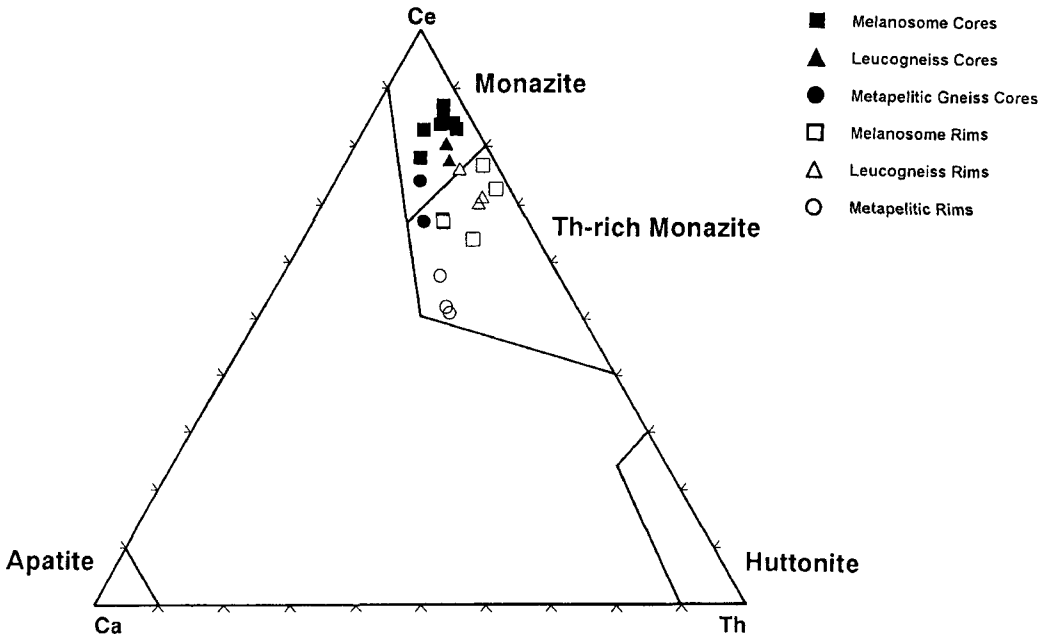

FIG. 2. Molecular Ce–Ca–Th plot, showing apatite ($CaPO_5$) and huttonite ($ThSiO_4$) composition fields (after Ward *et al.*, 1992). The monazite-(Ce) and high-Th monazite-(Ce) fields are adapted from Ward *et al.* (*op. cit.*) to reflect the compositional contrast between monazite-(Ce) rims and cores. Symbols: solid-fill — cores; white fill — rims; squares — melanosome; triangles — leucosome; circles — metapelitic gneisses. Cheralitic substitution of Th into rims is apparent.

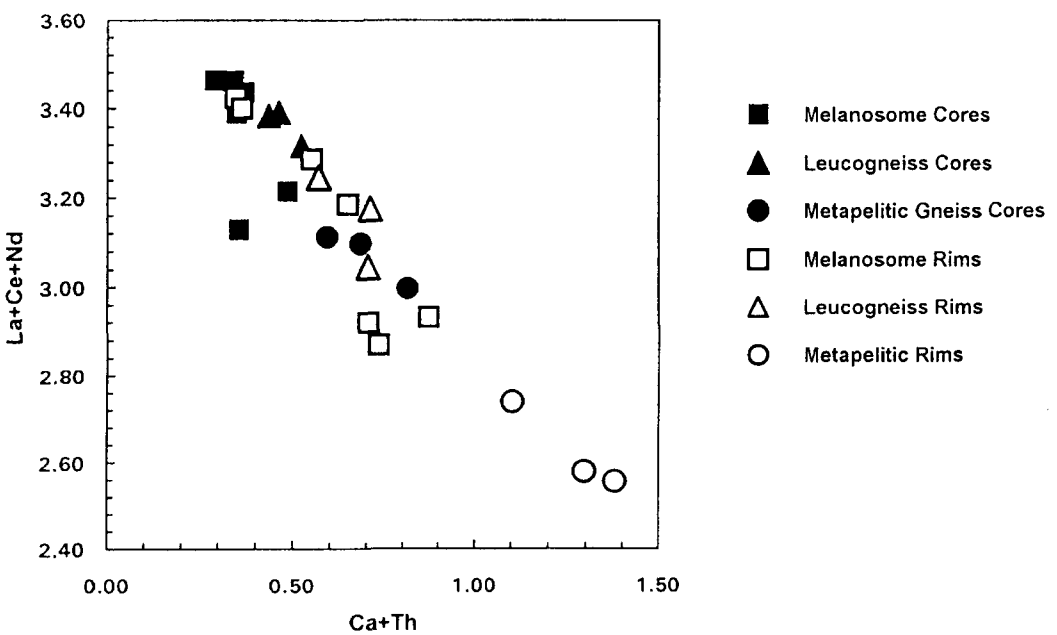

FIG. 3. Molecular La+Ce+Nd *vs.* Ca+Th plot showing strong negative correlation reflecting coupled substitution reaction 2. Symbols as Fig. 2.

mechanism. This mechanism alone, however, cannot explain the lower *REE* content of the monazite-(Ce) rims — some mechanism of retaining *LREE* in the melt while a Th-rich monazite-(Ce) precipitates is required.

Fluorine is an important species in many magmatic systems since HF will react with O^{2-} bridging ions, producing a dissociation analogous to the addition of H_2O (Burnham, 1979), resulting in lower melt viscosity. Fluorine partitions strongly into biotite over melt and volatile fluid. During incongruent partial melting of biotite, some F is released and dissolved in the melt. Biotites in the Brattstrand Bluffs migmatites, preserved in the cores of garnet, contain 3–5 wt.% F (Table 3). The addition of fluorine to the melt by the breakdown of this biotite during dehydration melting would lower melt viscosity and, more importantly, allow the formation of *REE*-fluorine complexes (Ponander and Brown, 1989). The formation of F-*REE* complexes would lower *REE* activities and result in reduced *REE* crystal–melt partition coefficients. One problem with this proposed mechanism, however, is the strong partitioning of F into biotite in preference to the melt. As biotite breakdown proceeds the F released will partition into any remaining biotite, thus stabilizng it to higher temperatures (Patiño-Douce and Johnston, 1991). Even if all biotite is consumed, the increased melt proportions may mean that absolute melt F-contents are no higher. The effect of absolute F-content on *REE*-fluorine complexing is not well documented in the literature, but if we accept that some of the F is released during biotite consumption then the increased Th contents of monazite-(Ce) rims, growing from a melt containing F, may have resulted from a decrease of *LREE* partitioning into monazite-(Ce). In addition, the increased substitution of Th into monazite-(Ce) would be enhanced during melting of metapelitic lithologies, since the liquids produced are highly silicic (Miller, 1985).

One final observation regarding the Th-rich rims found on all monazite-(Ce) grains in the Brattstrand Bluffs lithologies can be made. Watt and Harley (1993) presented a case for a melting model which involved the removal of melt from the melting zone before equilibration with the source. In effect, the low solubility of monazite in water-undersaturated melts prevented complete dissolution before melt extraction, leading to granitic liquids with low *LREE* contents similar to those described by Wickham (1987) and Sawyer (1991). No chemical zoning has been recorded in the Th-rich monazite-(Ce) rims. Diffusive homogenization cannot have occurred since palaeo-concentric zoning is evident in the cores (Fig. 1). If the monazite-(Ce) rims had grown in equilibrium with a melt with changing composition we would expect to see either step-like or smooth (Rayleigh-type) zoning profiles (e.g. Hinton and Paterson, 1994; Mohr, 1984) — the absence of zoning in the rims indicates that monazite-(Ce)-melt

TABLE 3. Biotite inclusions from the Brattstrand Bluffs Migmatites

Sample	75	98	56*	273*
Lithology	LG	LG	MPG	MPG
SiO_2	38.09	36.47	38.02	37.50
TiO_2	6.02	6.95	5.61	3.64
Al_2O_3	13.33	13.28	15.02	13.31
Cr_2O_3	n.a.	n.a.	0.07	0.08
FeO	8.97	10.17	9.35	13.77
MnO	0.01	0.02	0.01	0.02
MgO	17.41	15.78	16.65	15.39
ZnO	n.a.	n.a.	0.05	0.02
CaO	0.01	0.01	0.00	0.00
Na_2O	0.46	0.35	0.58	0.19
K_2O	9.49	8.91	9.80	8.98
F	4.83	4.27	4.03	3.50
O≡F	2.03	1.79	1.69	1.47
Total	96.59	94.42	97.50	94.93
Cations normalized (Si+Ti+Al+Cr+Fe+Mn+Mg+Zn) = 14				
Si	5.357	5.289	5.744	5.800
Ti	0.637	0.757	0.637	0.423
Al	2.210	2.270	2.675	2.428
Cr	–	–	0.008	0.010
Fe	1.055	1.233	1.181	1.783
Mn	0.001	0.002	0.001	0.002
Mg	3.650	3.411	3.749	3.552
Zn	–	–	0.005	0.002
Ca	0.002	0.002	0.000	0.000
Na	0.125	0.100	0.171	0.057
K	1.703	1.648	1.888	1.772
F	2.149	1.959	1.847	1.649
OH	0.000	0.284	1.469	2.026
O	21.688	21.600	20.684	20.325
X_{Mg}	0.78	0.73	0.76	0.67
X_K	0.93	0.94	0.92	0.96
X_{Fevi}	0.19	0.22	0.20	0.30
X_{OH}	0.00	0.12	0.44	0.55

* — Data from Fitzsimons, 1991

n.a. not analaysed
Biotite formula normalized to 14 [4] and [8] cations.
O = 20 × normalization factor
OH = 24-O-F
X_K K/Na+K
X_{Fevi} = Fe/6
X_{OH} = OH/(OH+F)

contact times were short and melt extraction rapid, consistent with the disequilibrium melting model of Watt and Harley (1993).

Conclusions

High-Th monazite-(Ce), previously recorded only in granitic pegmatites, has been noted in granulite-facies migmatites formed during water-undersaturated breakdown of biotite. Thorium contents in cores are typical of monazite found in granites (5–10 wt.% ThO_2), but rim compositions contain up to 21.4 wt.% ThO_2. Th enrichment in the rims of monazite-(Ce) in leucosomes, melansomes and migmatitic metapelitic gneisses is ascribed to the presence of F in water-undersaturated melts (formed during the incongruent breakdown of biotite), allowing the formation of *REE*-fluoride complexes in the melt. *REE* retention occurred in the melt, coupled with increased substitution of Si and Th via the charge-balanced substitution reactions $Th^{4+} + Si^{4+} \rightleftharpoons REE^{3+} + P^{5+}$ and $Th^{4+} + Ca^{2+} \rightleftharpoons 2REE^{3+}$ into monazite-(Ce), due to the high silica compositions of the melt. Fractionation of Th and U (reflected by an increase in Th/U in rims relative to cores) may have occurred due to removal by a CO_2-rich fluid phase in the melt. These interpretations are consistent with elevated CO_2 and fluorine contents of granitic liquids produced during the water-undersaturated breakdown of biotite under granulite-facies conditions, and may be widespread in granulite-facies migmatites. Rapid melt extraction, before equilibration of melt with residual solid, may be evidenced by the unzoned monazite-(Ce) rims.

Acknowledgements

I would like to acknowledge the receipt of an NERC PhD studentship at the University of Edinburgh, during which the monazite analyses were collected. The remaining work was carried out during a Research Fellowship at Oxford Brookes University. I am grateful to Stuart Kearns and Pete Hill of the Electron Microprobe Unit at the Department of Geology, University of Edinburgh, for their help with the monazite analyses, and to Anton Kearsley for his assistance in generating the X-Ray maps at Oxford Brookes University. Richard D'Lemos, Clarke Friend, Kev Jones, Tanya King and Ian Tribe are thanked for their thought-provoking comments and ideas on granite genesis and extraction, while Kelly Davis and Simon Deadman helped with the diagrams and plates. Finally, I would like to thank several members of E.A.S.I. (the East Antarctic Science Institute); namely, Simon Harley, Damian Carrington and Ian Fitzsimons, for their continuing support. Ian is also thanked for the biotite analyses given in Table 3.

References

Bowles, J.F.W., Jobbins, E.A. and Young, B.R. (1980) A re-examination of cheralite. *Mineral. Mag.*, **43**, 885–8.

Burnham, C.W. (1979) The importance of volatile constituents. In *The Evolution of the Igneous Rocks. Fiftieth Anniversary Perspectives* (H.S. Yoder, ed.), pp 439–82. Princeton University Press.

Demartin, F., Pilati, T., Diella, V., Donzelli, S. and Grammaccioli, C.M. (1991) Alpine monazite: further data. *Canad. Mineral.*, **29**, 61–7.

Feely, M., McCabe, E. and Williams, C.T. (1989) U-, Th- and REE-bearing accessory minerals in a high heat production leucogranite within the Galway granite, western Ireland. *Trans. Inst. Mining. Metall.*, **98**, 27–32.

Fitzsimons, I.C.W. (1991) *The Metamorphic Histories of some Proterozoic Granulites from East Antarctica.* PhD. thesis, University of Edinburgh, 375 pp. (Unpublished).

Fitzsimons, I.C.W. and Harley, S.L. (1991) Geological relationships in high-grade gneisses of the Brattstrand Bluffs coastline, Prydz Bay, east Antarctica. *Austral. J. Earth Sci.*, **38**, 497–519.

Gramaccioli, C.M. and Segalstad, T.M. (1978) A uranium- and thorium-rich monazite from a south-Alpine pegmatite at Piona, Italy. *Amer. Mineral.*, **63**, 757–61.

Harley, S.L. and Fitzsimons, I.C.W.(1991) Pressure–temperature evoluton of metapelitic granulites in a polymetamorphic terrane: the Rauer Group, east Antarctica. *J. Metam. Geol.*, **9**, 231–43.

Harley, S.L. and Hensen, B.J. (1990) Archaean and Proterozoic high-grade terranes of East Antarctica (40–80°E): a case study of diversity in granulite facies metamorphism. In *High Temperature Metamorphism and Crustal Anatexis.* (J.R. Ashworth and M. Brown, eds.). Unwin Hyman, London, 320–70.

Harley, S.L., Fitzsimons, I.C.W., Buick, I.S. and Watt, G.R. (1992) The significance of reworking, fluids and partial melting in granulite metamorphism, east Prydz Bay, Antarctica. In *Recent Progress in Antarctic Earth Science*, (Y. Yoshida, ed.). TERRAPUB, Tokyo, pp. 119–27.

Hensen, B.J. and Zhou, B. (1994) Two cycles of granulite facies metamorphism detected by Sm-Nd dating of garnet: implications for the Sm-Nd closure temperature. *Mineral. Mag.*, **58A**, 412–3.

Hinton, R.W. and Paterson, B.A. (1994) Crystallisation history of granitic magma: evidence from trace element zoning. *Mineral. Mag.*, **58a**, 416–7.

Keppler, H. and Wyllie, P.J. (1990) Role of fluids in

transport and fractionation of uranium and thorium in magmatic processes. *Nature*, **348**, 531–3.

Keppler, H. and Wyllie, P.J. (1991) Partitioning of Cu, Sn, Mo, W, U and Th between melt and aqueous, fluid in the systems haplogranite–H_2O–HCl and haplogranite–H_2O–HF. *Contrib. Mineral. Petrol.*, **109**, 139–50.

Mannucci, G., Diella, V., Grammacioli, C.M. and Pilati, T.(1986) A comparative study of some pegmatitic and fissure monazite from the Alps. *Canad. Mineral.*, **24**, 469–74.

Miller, C.F. (1985) Are strongly peraluminous magmas derived from pelitic sedimentary sources. *J. Geol.*, **9**, 673–89.

Miller, C.F., Mittlefehldt, D.W. (1983) Geochemistry of the Sweetwater Wash Pluton, California: implications for 'anomalous' trace element behaviour during differentiation of felsic magmas. *Geochim. Cosmochim. Acta*, **47**, 109–24.

Mohr, D.W. (1984) Zoned porphyroblasts of metamorphic monazite-(Ce) in the Anakeesta Fmn. Great Smoky Mountains, North Carolina. *Amer. Mineral.*, **69**, 98–103.

Montel, J.M. (1993) A model for monazite/melt equilibrium and application to the generation of magmas. *Chem. Geol.*, **100**, 127–46.

Mysen, B.O. and Virgo, D. (1985) Structure and properties of fluorine bearing aluminosilicate melts: the system Na_2O–Al_2O_3–SiO_2–F at 1 atm. *Contrib. Mineral. Petrol.*, **91**, 205–20.

Patiño-Douce A.E. and Johnston, A.D. (1991) Phase equilibria and melt productivity in the pelitic system: implications for the origin of peraluminous granitoids and aluminous granulites. *Contrib. Mineral. Petrol.*, **107**, 202–18.

Ponander, C.W. and Brown, G.E. Jr (1989) Rare earth elements in silicate glass/melt systems: II. Interactions of La, Gd and Yb with halogens. *Geochim. Cosmochim. Acta*, **53**, 2905–14.

Sawka, W.N., Chappell, B.W. and Norrish, K. (1984) Light-rare-earth-element zoning in sphene and allanite during granitoid fractionation. *Geology*, **12**, 131–4.

Sawyer, E.W. (1991) Disequilibrium melting and the rate of melt-residuum separation during migmatisation of mafic rocks from the Grenville Front, Quebec. *J. Petrol.*, **32**, 701–38.

Sevigny, J.H. (1993) Monazite controlled Sm/Nd fractionation in leucogranites: An ion microprobe study of garnet phenocrysts. *Geochim. Cosmochim. Acta*, **57**, 4095–102.

Ward, C.D., McArthur, J.M. and Walsh, J.N. (1992) Rare earth element behaviour during evolution and alteration of the Dartmoor Granite, SW England. *J. Petrol.*, **33**, 785–815.

Ward, D.A. and Miller, C.F. (1993) Accessory mineral behaviour during differentiation of a granite suite: monazite, xenotime and zircon in the Sweetwater Wash pluton, southeastern California, U.S.A. *Chem. Geol.*, **110**, 49–67.

Watt, G.R. and Harley, S.L. (1993) Accessory phase controls on the geochemistry of crustal melts and restites produced by dehydration melting. *Contrib. Mineral. Petrol.*, **114**, 550–66.

White, A.J.R. (1990) *A workshop on Crustal Protoliths of Granites*. Course Notes, Department of Geology, University of St Andrews, St Andrews, Scotland.

Wickham, S.M. (1987) The segregation and emplacement of granitic magmas. *J. Geol. Soc.*, **144**, 281–97.

Zhao, J.X. and Cooper, J.A. (1993) Fractionation of monazite in the development of V-shaped REE patterns in leucogranite systems: Evidence from a muscovite leucogranite body in central Australia. *Lithos*, **30**, 23–32.

[*Manuscript received 11 November 1994: revised 15 February 1995*]